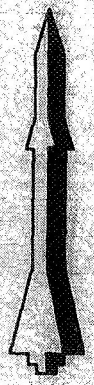

REPORT 70–5

SUMMARY OF COMBUSTION INSTABILITY RESEARCH

Conducted During August 1, 1969 – July 31, 1970

At the Georgia Institute of Technology

B. T. Zinn, W. C. Strahle, E. A. Powell, M. E. Lores

AUGUST 1970

prepared for

National Aeronautics and Space Administration

NASA Lewis Research Center
Grant NGR 11–002–083
Dr. R. J. Priem, Project Manager
Chemical Rockets Division

GITAER 70 – 5

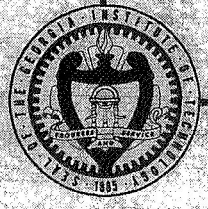

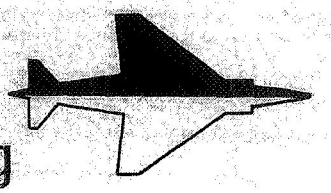

School of Aerospace Engineering
GEORGIA INSTITUTE OF TECHNOLOGY
Atlanta, Georgia 30332

REPORT 70-5

SUMMARY OF COMBUSTION INSTABILITY RESEARCH

Conducted During August 1, 1969 - July 31, 1970

At the Georgia Institute of Technology

B. T. Zinn, W. C. Strahle, E. A. Powell, M. E. Lores

August 1970

prepared for

National Aeronautics and Space Administration

NASA Lewis Research Center
Grant NGR 11-002-083
Dr. R. J. Priem, Project Manager
Chemical Rockets Division

ABSTRACT

The status and summary of recent results obtained in various studies aimed at developing means for a priori predicting the nonlinear behavior of unstable liquid-propellant rocket motors are described. The studies under consideration include: (1) Determination of the nonlinear behavior of unstable rockets with the aid of a second order theory; (2) The development of a third order theory; (3) Investigation of nonlinear axial instability in liquid rockets; and (4) Investigation of the behavior of the unsteady combustion response function.

SUMMARY

Brief descriptions of combustion instability studies performed at Georgia Institute of Technology during the second year of financial support under NASA grant NGR 11-002-083 are provided.

This project is concerned with the application of the Galerkin method in the prediction of the nonlinear behavior of unstable liquid-propellant rocket motors. In a study of transverse instabilities, numerical results predicting stable limit cycles, triggering limits, and nonlinear pressure waveforms were obtained. The dependence of the engine's nonlinear stability characteristics upon various engine parameters was also studied. The importance of various types of nonlinearities present in the conservation equations was also investigated.

During this same period investigation of the nonlinear axial mode instability problem was continued. Three approximate methods of solution have been devised, and computer programs based on these methods are presently being developed.

A study of the behavior of the unsteady combustion response function was also initiated during this period.

INTRODUCTION

During the first year of NASA support for this project an approximate mathematical technique was successfully applied in the solution of a number of combustion instability problems[1]. Special attention was given to the study of nonlinear effects. As part of this effort a nonlinear second-order theory, which formed the basis for a computer program designed to predict the nonlinear behavior of unstable liquid propellant rocket motors, was developed.

The work performed during the second year of this project represents an extension and diversification of the research performed during the first year. Several different aspects of nonlinear combustion instability were considered and the following investigations were conducted: (1) the study of moderate amplitude transverse instability based on the second order theory developed during the first year, (2) the development and application of a third order theory to study large amplitude transverse instabilities, (3) the study of nonlinear axial mode instability, and (4) the study of the behavior of unsteady combustion response functions.

Some of the results obtained with the aid of the second order theory were presented at the 6th ICRPG Combustion Conference held in Chicago during September 9-11, 1969. Additional results appear in the following publications:

(1) Powell, E. A., and Zinn, B. T., "Nonlinear Combustion Instability in Liquid-Propellant Rocket Engines," published in the Proceedings of the 6th ICRPG Combustion Conference, December 1969, pp. 199-208.

(2) Powell, E. A., "Nonlinear Combustion Instability in Liquid Propellant Rocket Engines," Georgia Institute of Technology,

Department of Aerospace Engineering, (Ph.D. Thesis), 1970.

(3) Strahle, W. C., "A Note on the Forgotten Velocity Effect in Combustion Instability of Liquid Rockets," accepted for publication in Combustion Science and Technology.

(4) Strahle, W. C., "New Considerations on Causes for Combustion Instability in Liquid Propellant Rockets," accepted for publication in Combustion Science and Technology.

The following paper has been accepted for presentation (and for publication in the proceedings of the conference) at the Thirteenth International Symposium on Combustion, to be held at the University of Utah during August 23-29, 1970:

Zinn, B. T., and Powell, E. A., "Nonlinear Combustion Instability in Liquid Propellant Rocket Engines."

Brief description of the results obtained in the above-mentioned investigations are provided in the following sections. These sections are followed by a brief description of proposed future research.

Results of the Second Order Transverse Instability Studies

During the first year of this project it was shown[6] that when the mean flow Mach number is small the wave motion inside the combustor of a liquid-propellant rocket engine can be described, to second order, by the following nonlinear partial differential equation:

$$\nabla^2\Phi - \Phi_{tt} = 2\vec{u}\cdot\nabla\Phi_t + \gamma(\nabla\cdot\vec{u})\Phi_t$$

$$+ 2\nabla\Phi\cdot\nabla\Phi_t + (\gamma-1)\Phi_t\nabla^2\Phi + W_m' \qquad (1)$$

In the above equation, Φ is the velocity potential defined by $\underset{\rightarrow}{V}' = \nabla\Phi$, $\underset{\rightarrow}{\bar{u}}$ is the steady state velocity, and W_m' is the mass source perturbation that results from the unsteady response of the burning process to the pressure oscillations. This section presents a summary of the results obtained when Eq. (1) was used to study the nonlinear stability characteristics of cylindrical combustion chambers in which the liquid propellants are injected uniformly across the injector face and the combustion process is distributed throughout the combustion chamber. Crocco's time-lag hypothesis was used to describe the unsteady combustion process; hence the unsteady mass source is given by:

$$W_m' = - \gamma n \frac{d\bar{u}}{dz} \left[\Phi_t(r,\theta,z,t) - \Phi_t(r,\theta,z,t - \bar{\tau}) \right] \qquad (2)$$

where n is the pressure interaction index and $\bar{\tau}$ is the steady state value of the time-lag. It was also assumed that the hot combustion products leave the combustion chamber through a multi-orifice quasi-steady nozzle.

In order to study transverse combustion instability, an approximate solution for the velocity potential was constructed as a series expansion in the tangential acoustic modes, and each of these modes was multiplied by an undetermined time-dependent coefficient. Using this series expansion and following the mathematical procedure outlined in Ref. 2 the solution of the original partial differential equation was reduced to the solution of a system of coupled nonlinear ordinary differential equations that control the behavior of the unknown time-dependent amplitudes. These equations form the basis of a computer program for calculating the nonlinear transverse stability characteristics of liquid propellant rocket engines.

Extensive numerical computations using series solutions containing various combinations of the chamber's natural modes were performed. The calculated results indicated that a series expansion consisting of the first tangential (1T), second tangential (2T), and first radial (1R)

modes provides a good description of the engine stability characteristics. Thus the velocity potential was approximated by the following series expansion:

$$\tilde{\Phi} = B_{01}(t)J_0(S_{01}r) + \left[A_{11}(t)\sin\theta + B_{11}(t)\cos\theta\right]J_1(S_{11}r) + \left[A_{21}(t)\sin 2\theta + B_{21}(t)\cos 2\theta\right]J_2(S_{21}r) \qquad (3)$$

Numerical calculations obtained using the above three-mode series are presented with the following objectives in mind: (1) the prediction of the final amplitude for transverse mode instability; (2) the determination of the waveform and frequency of the nonlinear oscillations; and (3) the determination of the dependence of the resulting oscillation upon (a) the initial disturbance, (b) the combustion parameters n and $\bar{\tau}$, (c) the magnitude of the steady state Mach number at the nozzle entrance, and (d) the combustor's length-to-diameter ratio.

For a given initial disturbance it was possible to follow the time evolution of the three modes included in the series expansion. The computations showed that in the region of the (n, $\bar{\tau}$) plane where the 1T mode is the only linearly unstable mode in the series (i.e., Region I of Fig. 1) an initial disturbance develops into a finite-amplitude oscillation. The magnitude of the final amplitude depends on the nature of the initial disturbance (i.e., spinning or standing) but not on the magnitude of the initial disturbance. These studies showed that in this region of the (n, $\bar{\tau}$) plane, the magnitude of the final amplitude is limited by nonlinear coupling between modes, whereby energy is transferred from the linearly unstable 1T mode to the linearly stable modes (2T and 1R). More complex behavior was observed in regions of the (n, $\bar{\tau}$) plane where the 1R mode is unstable and the 1T mode is either stable or unstable. In such regions (i.e., Region III of Fig. 1) "back-and-forth" energy transfer between the modes produces a finite-amplitude, highly-modulated oscillation which exhibits some character-

istics of both modes.

As seen in Fig. 2, once a stable limit cycle is reached the time dependent coefficients (i.e., mode-amplitudes) appearing in Eq. (3) are nearly sinusoidal functions of time. In most of the cases computed the 1R and 2T modes had a much smaller amplitude than the 1T mode and were oscillating at twice the frequency of the 1T mode. Using the mode-amplitudes the nonlinear pressure waveforms at any location in the chamber were easily computed. Typical wall pressure waveforms for standing 1T oscillations are shown in Figs. (3) and (4). These waveforms exhibit a pronounced second harmonic distortion, resulting in sharp peaks and shallow minima. Also predicted is a small-amplitude, double-frequency oscillation at the locations for the (1T) pressure nodes (i.e., $\theta = 0$ and $\theta = \pi$).

The predicted dependence of the final amplitude upon the combustion parameters n and $\bar{\tau}$ is shown in Fig. (5) for a standing type instability. In this plot δ is the displacement of the operating point $(n, \bar{\tau})$ from the neutral stability limit measured along a line of constant $\bar{\tau}$. Positive values of δ indicate displacements into the linearly unstable region. From this figure it is seen that the limiting amplitude increases with both increasing vertical displacement (i.e., increasing the value of n) and with increasing time-lag. For the 1T spinning instability similar plots were obtained, and they are compared with those for standing oscillations in Fig. (6). In most of the cases considered an initially spinning wave disturbance resulted in instabilities with larger final amplitude oscillations. The frequency of oscillation was also found to depend on n and $\bar{\tau}$. As seen from Fig. (7) the frequency decreases with increasing amplitude (i.e., increasing n) and with increasing $\bar{\tau}$. The above results were used to construct nonlinear $(n, \bar{\tau})$ stability maps (see Fig. (8)) showing the dependence of the final amplitude upon the values of n and $\bar{\tau}$.

The second order theory was also used to determine the dependence of the final amplitude upon the engine's mean flow as well as the engine's

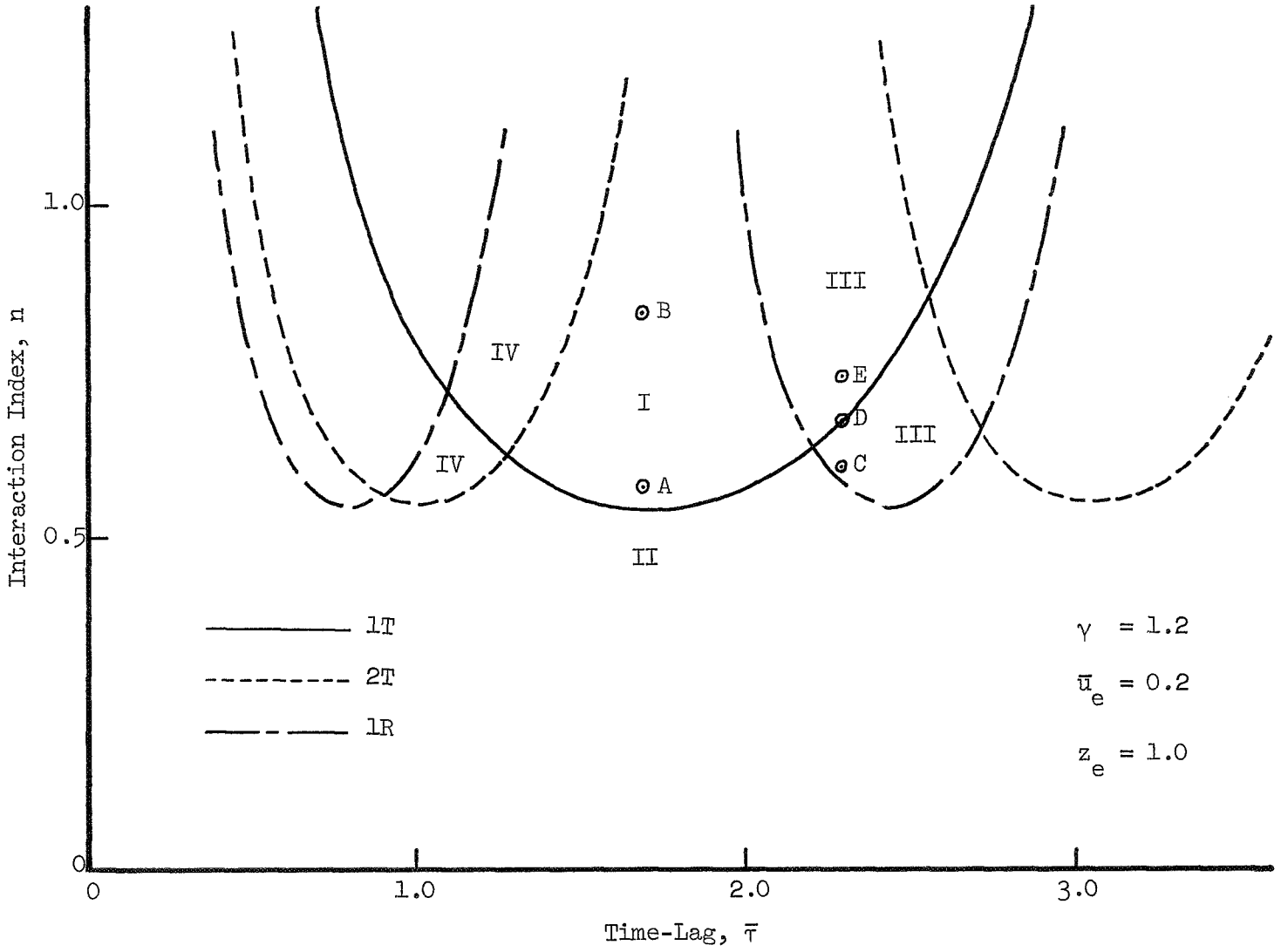

Figure 1. Regions of Interest in the Stability Plane.

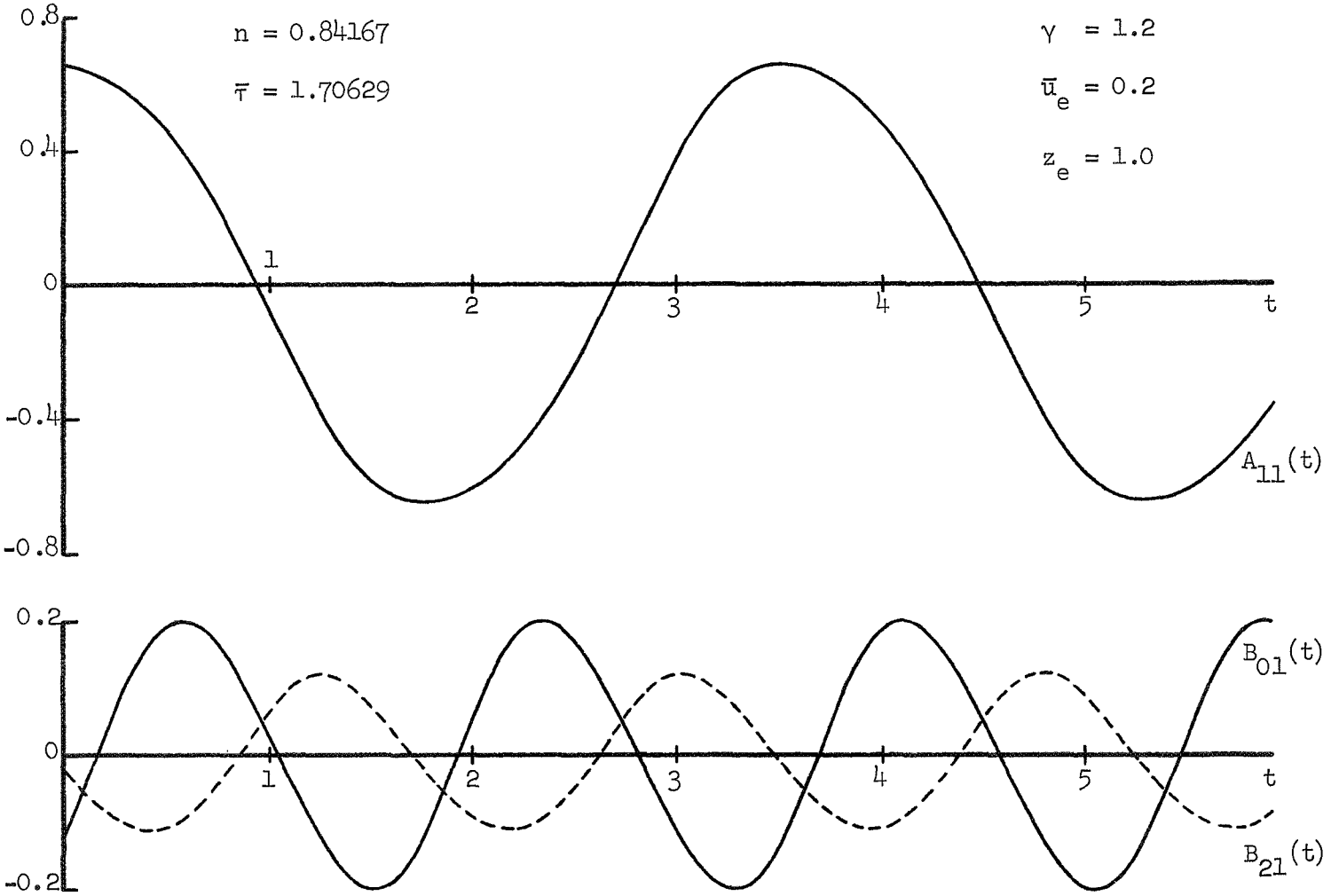

Figure 2. Time Dependence of the Mode-Amplitude Functions at a Stable Limit Cycle.

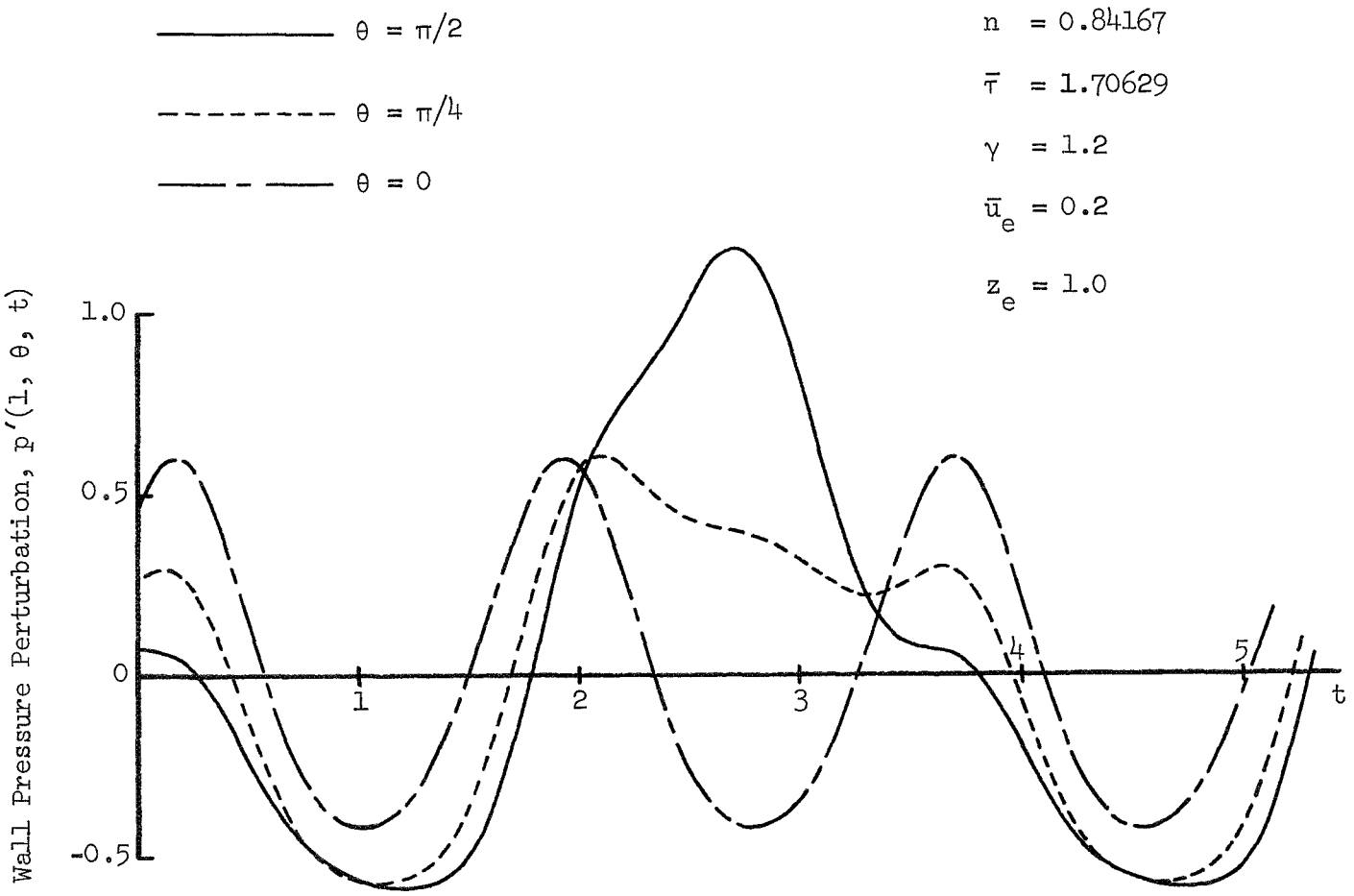

Figure 3. Time Dependence of the Wall Pressure Waveforms for a Large Amplitude Standing 1T Oscillation.

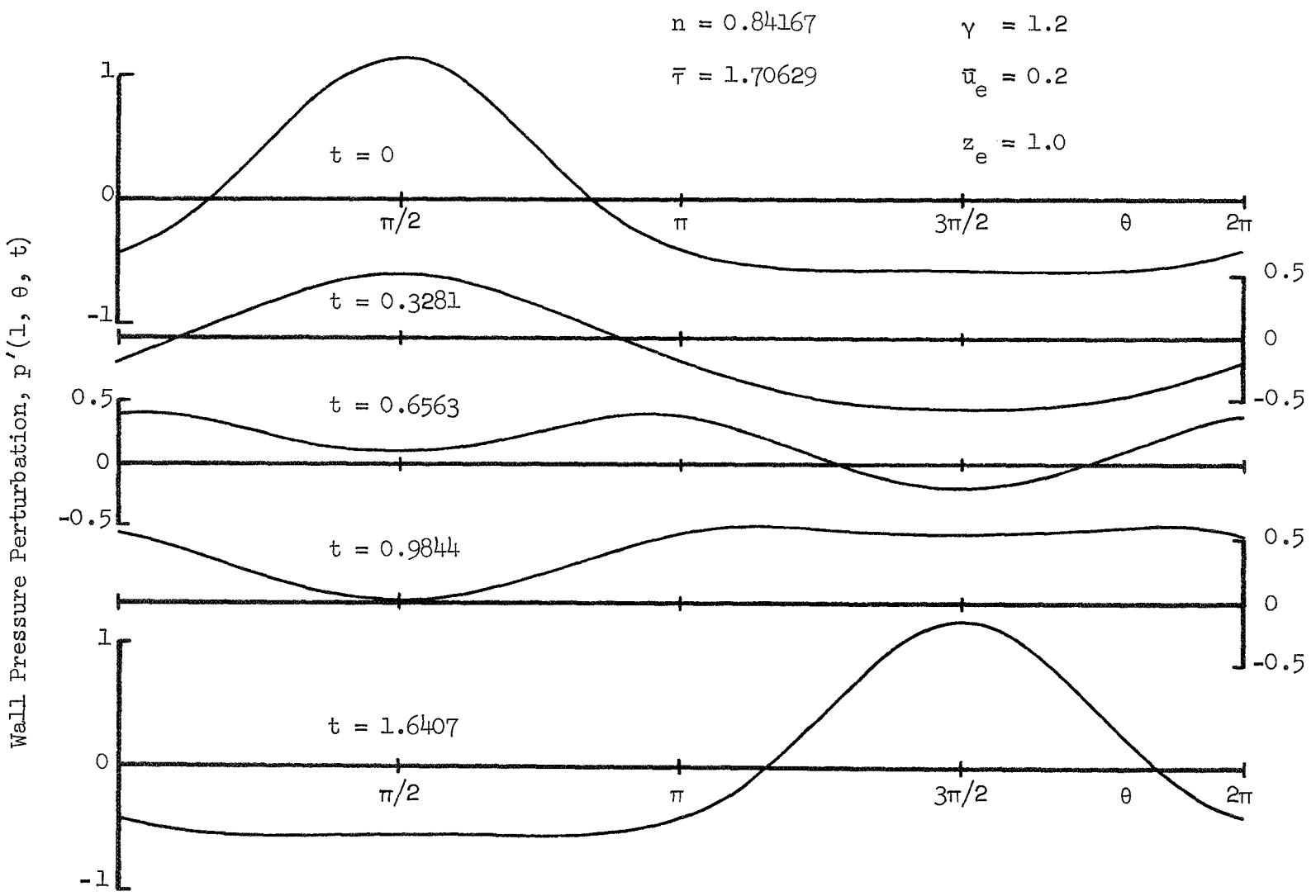

Figure 4. Angular Dependence of the Wall Pressure Waveforms for a Large Amplitude Standing 1T Oscillation.

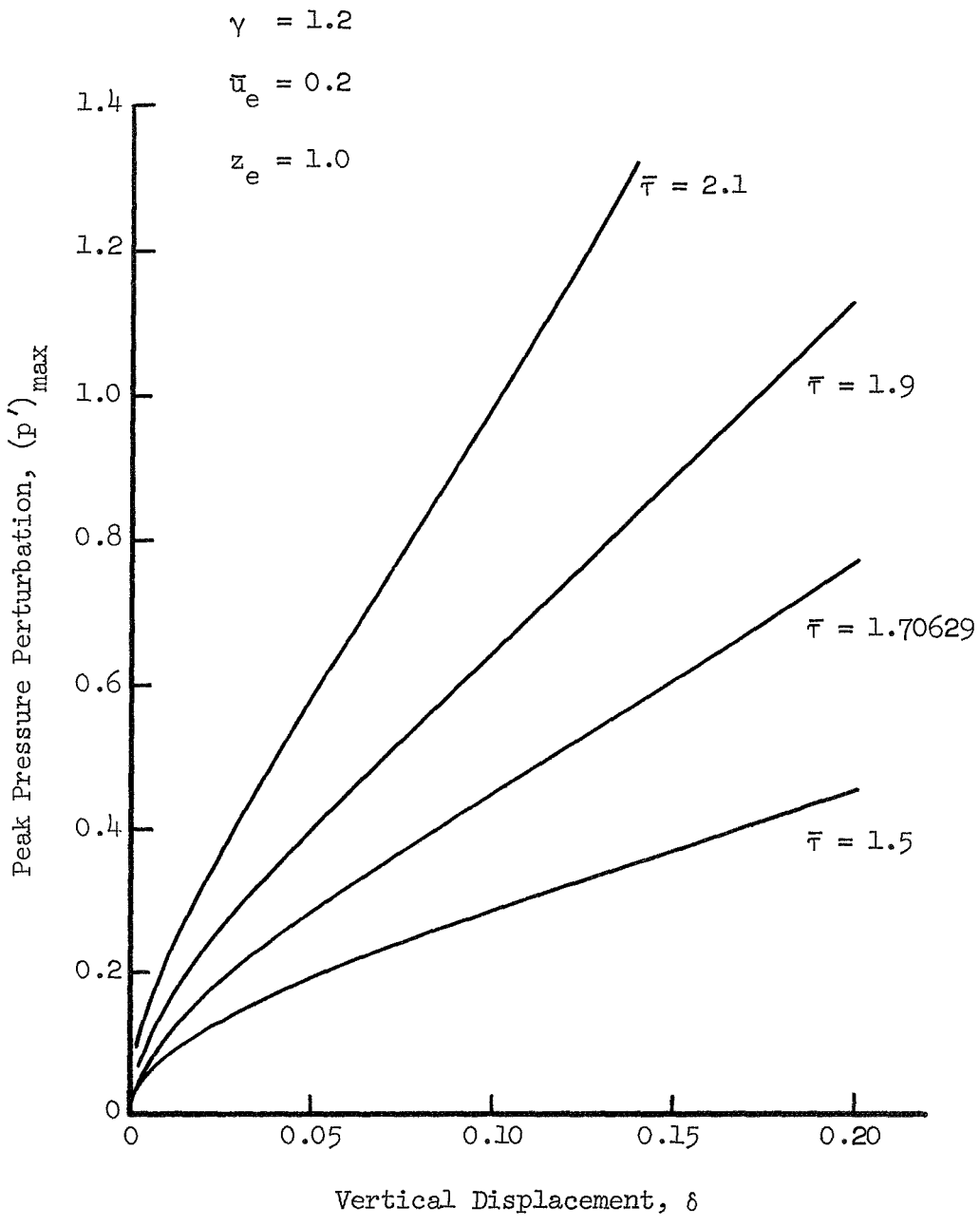

Figure 5. Dependence of the Limiting Pressure Amplitude Upon Combustion Parameters.

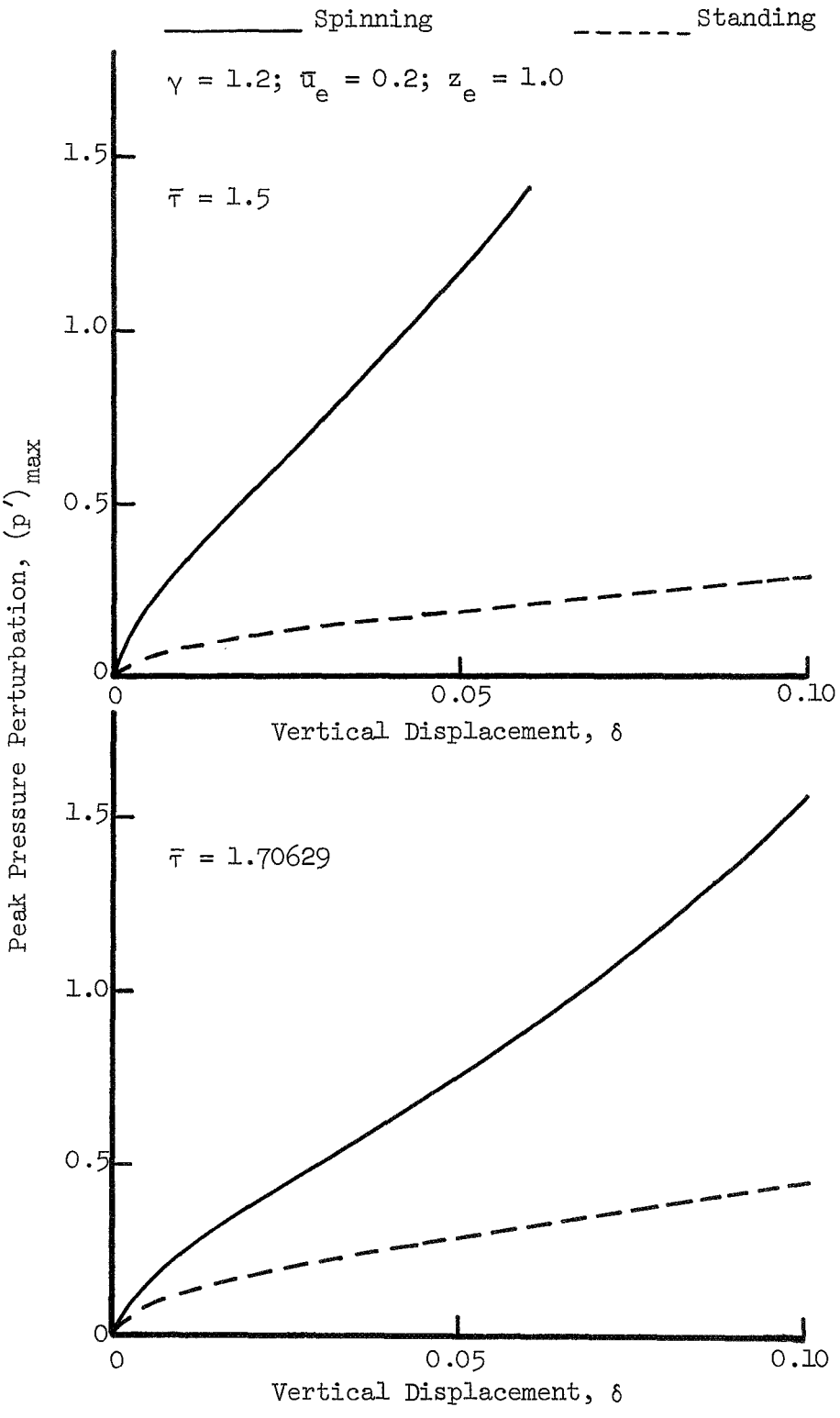

Figure 6. Comparison of the Limiting Pressure Amplitude for Spinning and Standing Type Instabilities.

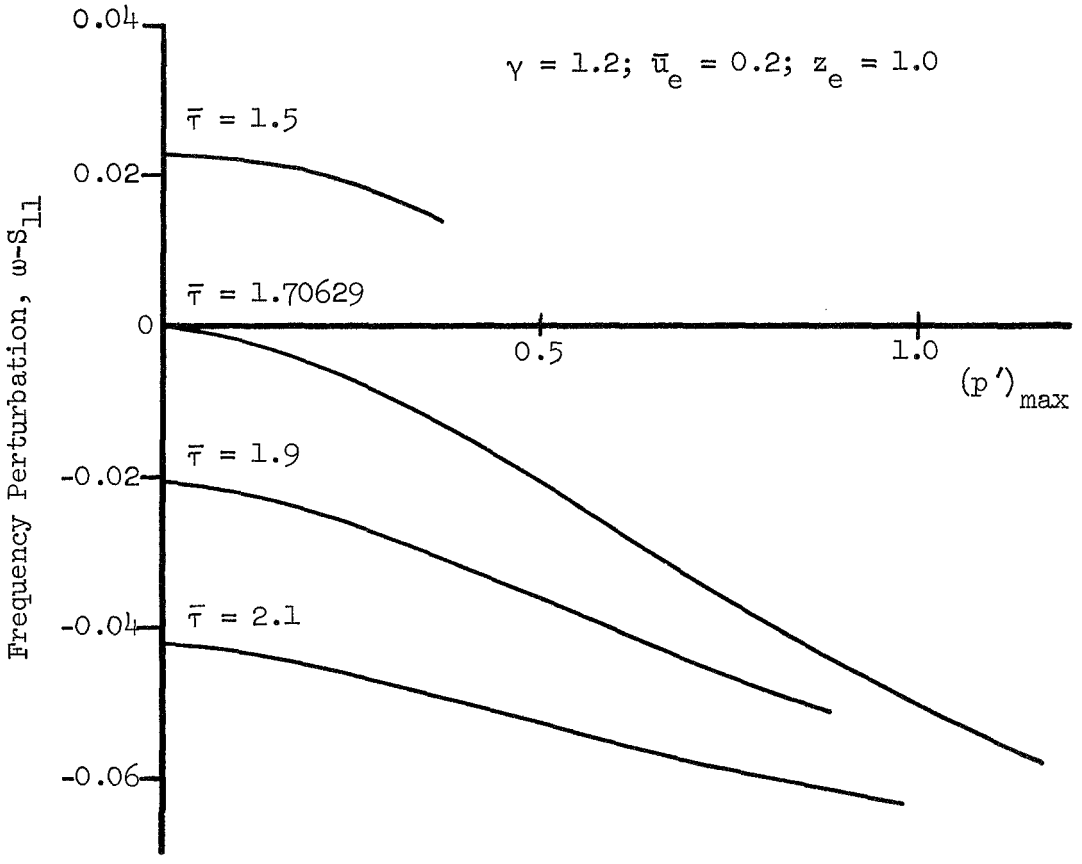

Figure 7. Dependence of the Frequency upon the Amplitude for Standing Type Instabilities.

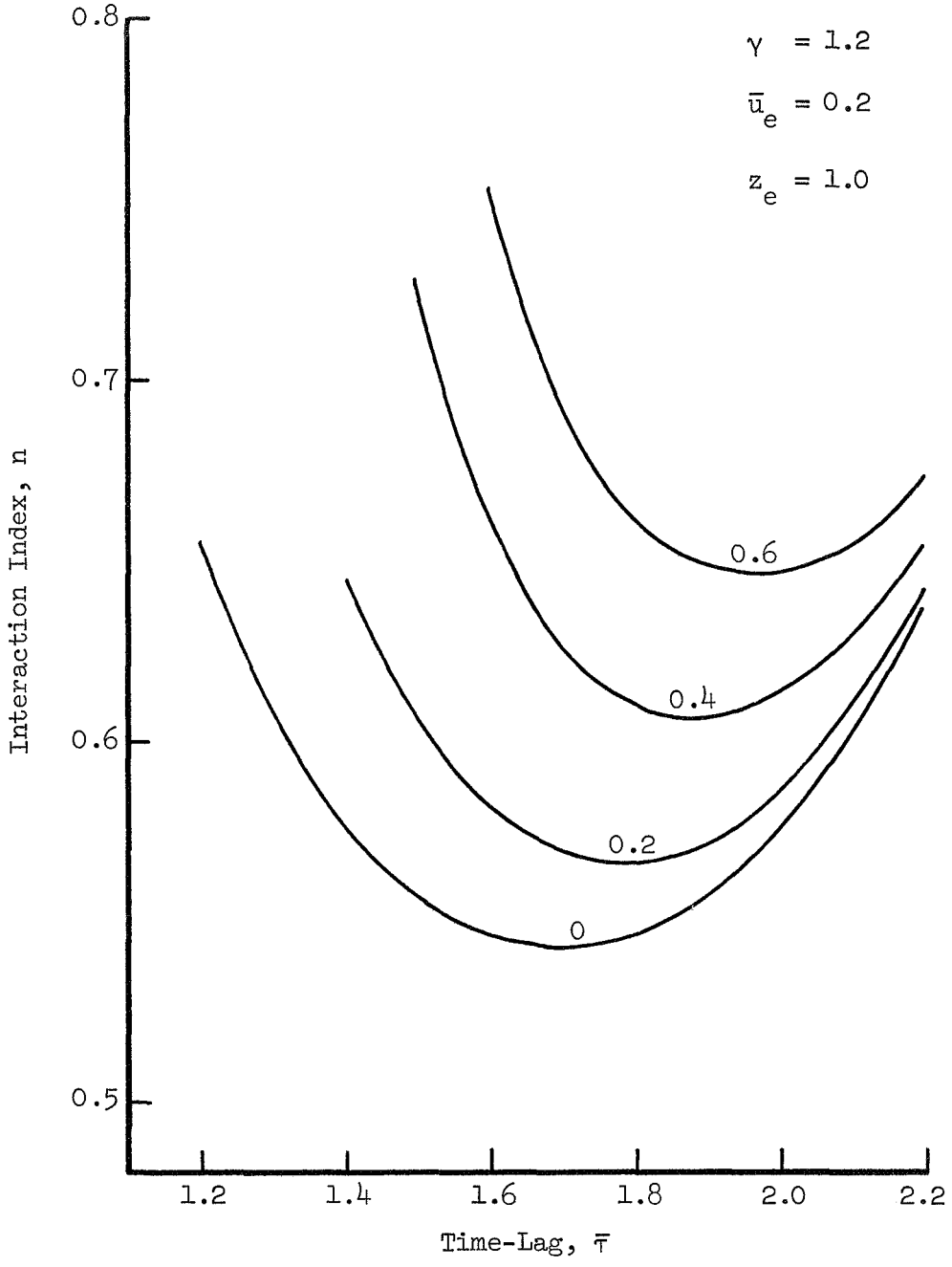

Figure 8. Stability Map with Curves of Constant Pressure Amplitude.

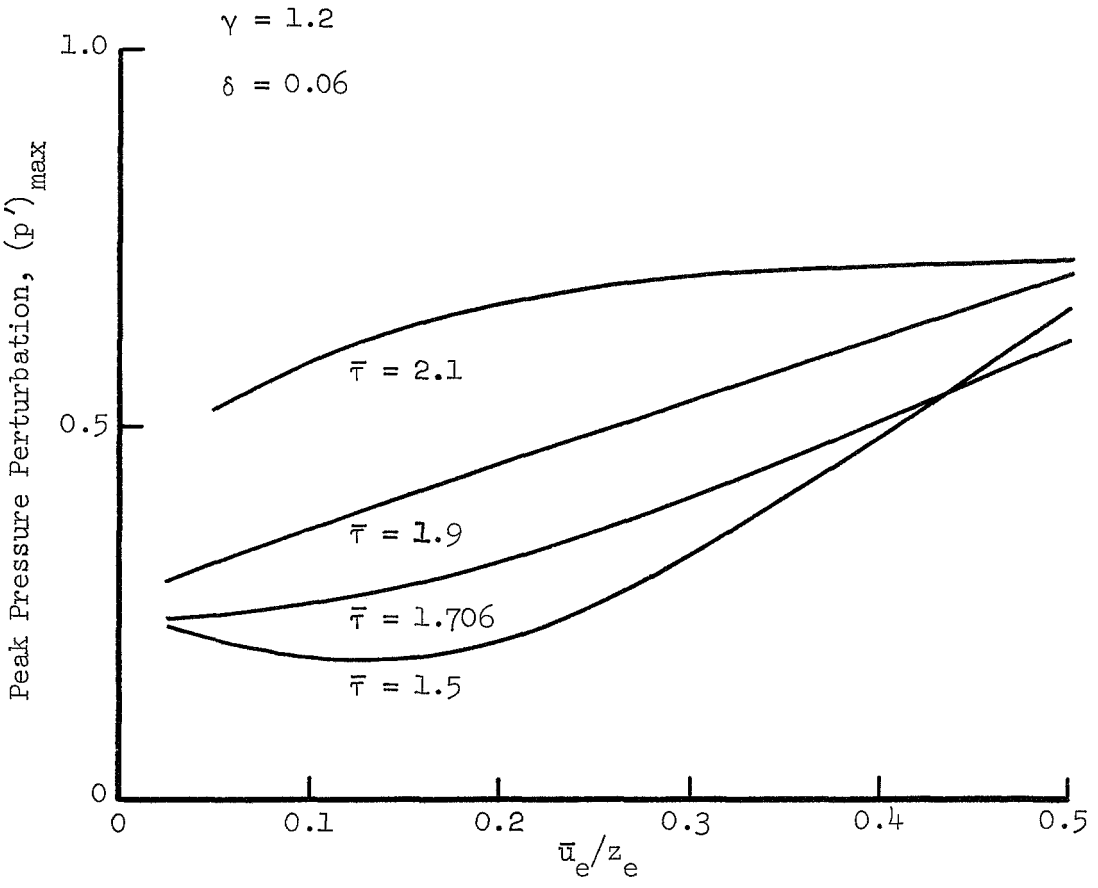

Figure 9. Dependence of the Limiting Pressure Amplitude upon the Ratio $\bar{u}_e/z_e$.

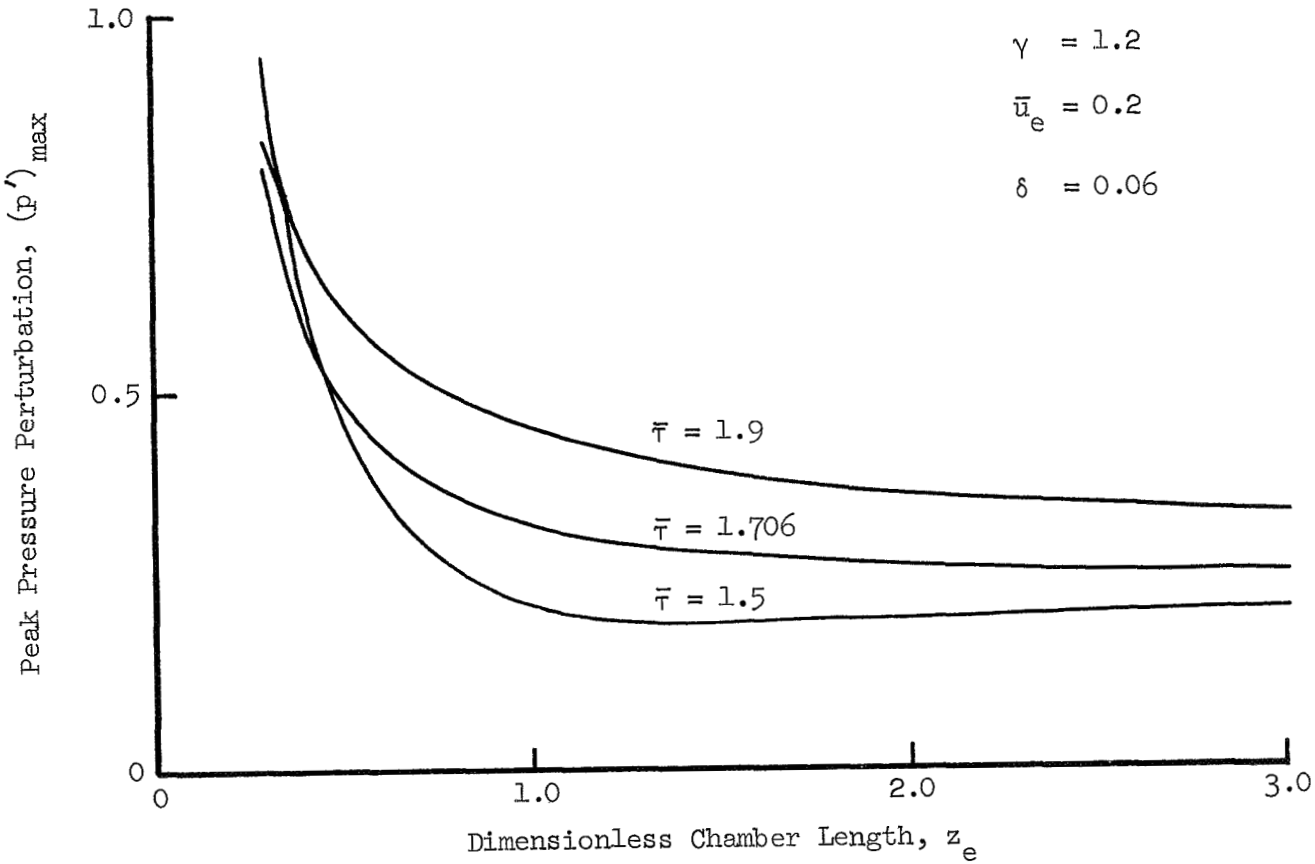

Figure 10. Effect of Chamber Length upon the Limiting Pressure Amplitude.

length. In these studies the values of n and $\bar{\tau}$ were held fixed and the unstable behavior for various values of $\bar{u}_e$ (i.e., Mach number at the nozzle entrance) and z_e (i.e., dimensionless length) was investigated. The results of this study are shown in Figs. (9) and (10). It is seen from Fig. (9) that an increase in $\bar{u}_e$ usually resulted in an increase in the limiting pressure amplitude; the exception occurring at smaller values of $\bar{\tau}$. Figure (10) shows that for fixed values of n, $\bar{\tau}$, and $\bar{u}_e$ increasing the length z_e resulted in a decrease in the limiting value of the pressure amplitude.

Third Order Transverse Investigations

During the second year of this project a third order theory was developed. This theory represents an attempt to relax some of the restrictions imposed on the second order theory. The latter included such restrictions as small Mach number mean flow, irrotationality of the flow, and the presence of moderate amplitude waves. In the third order analysis no terms were neglected in the conservation equations; the only approximations used being those related to the absence of droplet drag and constancy of droplet stagnation enthalpy, both of which were used in the second order theory.

Under the above assumptions the conservation equations can no longer be combined to obtain a single equation governing the behavior of the velocity potential. Instead a system of partial differential equations must be solved. The development of these equations will now be briefly described. Considering only transverse oscillations the velocity components can be defined as follows:

$$v' = \frac{\partial \eta}{\partial r} \quad ; \quad w' = \frac{1}{r}\frac{\partial \zeta}{\partial \theta} \tag{4}$$

where v' and w' respectively represent the radial and tangential velocity components and η and ζ are quasi-potentials. Using Eqs. (4) the appropriate system of conservation equations becomes:

Continuity:

$$\frac{\partial \rho'}{\partial t} + \left[\bar{\rho}(z) + \rho'\right]\left[\eta_{rr} + \frac{1}{r}\eta_r + \frac{1}{r^2}\zeta_{\theta\theta}\right] \tag{5}$$

$$+ \eta_r \rho_r' + \frac{1}{r^2}\zeta_\theta \rho_\theta' + \rho' \frac{d\bar{u}}{dz} - W_m' = 0$$

Radial momentum:

$$(\bar{\rho} + \rho')\left[\eta_{rt} + \eta_r \eta_{rr} + \frac{1}{r^2}\zeta_\theta \eta_{r\theta} - \frac{1}{r^3}\zeta_\theta^2\right] + \frac{1}{\gamma} p_r' = 0 \tag{6}$$

Tangential momentum:

$$(\bar{\rho} + \rho')\left[\zeta_{\theta t} + \eta_r \zeta_{r\theta} + \frac{1}{r^2}\zeta_\theta \zeta_{\theta\theta}\right] + \frac{1}{\gamma} p_\theta' = 0 \tag{7}$$

Energy:

$$(\bar{\rho} + \rho')\left[\frac{\partial h_s'}{\partial t} + \eta_r \frac{\partial h_s'}{\partial r} + \frac{1}{r^2}\zeta_\theta \frac{\partial h_s'}{\partial \theta}\right] - \frac{\gamma - 1}{\gamma}\frac{\partial p'}{\partial t} + \frac{d}{dz}(\bar{\rho}\bar{u}) h_s' + W_m' h_s' = 0 \tag{8}$$

Equation of State:

$$p' = \bar{\rho} h_s' + \rho' \bar{h}_s + \rho' h_s' - \frac{\gamma - 1}{2}\left[(\bar{\rho} + \rho')\left(\eta_r^2 + \frac{1}{r^2}\zeta_\theta^2\right) + \rho' \bar{u}^2\right] \tag{9}$$

In the above equations ρ is the density, p is the pressure, and h_s is the stagnation enthalpy.

To complete the theory higher order expressions for the burning rate term and nozzle admittance relation are needed. Unlike the expressions describing the gas dynamics of the problem these expressions

contain terms of all orders and they need to be truncated to include terms up to third order only. In deriving these expressions it was assumed that the combustor's mean flow Mach number was small. Using Crocco's time-lag hypothesis the third order burning rate expression is given by the following expression:

$$W'_m = n \frac{d\bar{u}}{dz} \left\{ (p' - p'_\tau) + \frac{n-1}{2} (p')^2 - n\, p'\, p'_\tau \right.$$

$$\left. + \frac{n+1}{2} (p'_\tau)^2 - n \frac{\partial p'_\tau}{\partial t} \int_{t-\bar{\tau}}^{t} p'(t')dt' \right\} \qquad (10)$$

where $p'_\tau = p'(r,\theta,t-\bar{\tau})$.

Due to the complexity of Eqs. (5) through (9), the nonlinear behavior of a single transverse mode was investigated by approximating each dependent variable as the product of an amplitude function and the spatial dependence of that mode. The approximate solutions are expressed in the following form:

$$\tilde{\rho}' = A_\rho(t)\Psi_{mn}(r,\theta)$$

$$\tilde{\eta} = A_\eta(t)\Psi_{mn}(r,\theta)$$

$$\tilde{\zeta} = A_\zeta(t)\Psi_{mn}(r,\theta)$$

$$p' = A_p(t)\Psi_{mn}(r,\theta)$$

$$h'_s = A_h(t)\Psi_{mn}(r,\theta) \qquad (11)$$

where $\Psi_{mn}(r,\theta) = \cos m\theta J_m(S_{mn}r)$. Introducing the approximate solutions into Eqs. (5) through (9) and applying the mathematical technique described in Ref. 2 yields a system of nonlinear ordinary differential equations to be solved for the unknown A's. A computer program was developed to determine these amplitude functions numerically.

As a check on the analysis, linear stability limits were computed using the linearized version of the system of equations derived for the third order theory. Except for small corrections of the order of $\bar{u}_e^2$ these limits agreed with those computed from the linearized version of the second order theory.

Using the third order theory numerical solutions were obtained for the following two cases: (1) the approximate solutions consisted of the first tangential mode only, and (2) the approximate solutions consisted of the first radial mode only. The systems of differential equations governing these two cases differed in several respects. The equations governing the behavior of the 1R mode contained both quadratic and cubic nonlinearities while those describing the behavior of the 1T mode contained only cubically nonlinear terms. The radial mode equations also contained nonlinearities in the combustion mass source terms whereas a nonlinear driving term did not appear in the equations for the 1T mode.

The numerical results show that the above-mentioned differences are important. The important characteristics of the 1T mode solutions will now be summarized. As seen from Fig. (11) the pressure and velocity waveforms are nearly sinusoidal in shape, a result in contrast to the results of the second order theory. The effect of the combustion parameters n and $\bar{\tau}$ upon the final amplitude of the pressure oscillation is shown in Figs. (12) and (13). For values of $\bar{\tau} \leq 2.1$ in the linearly unstable region, stable limit cycles were found as shown in Fig. (12). In each case the final amplitude attained for given values of n and $\bar{\tau}$ was considerably larger than the amplitude predicted by the second order theory. The possibility of "triggering" combustion oscillations

was found to exist for $\bar{\tau} > 2.1$. Figure (13) shows the dependence of the triggering amplitude with n and $\bar{\tau}$ for standing 1T initial disturbances. For given values of n and $\bar{\tau}$ an initial disturbance with amplitude slightly less than the threshold value, given by the curve, will decay to zero amplitude. No stable limit cycles could be found in this region. A disturbance with amplitude slightly above the critical value was found to grow without limit. The differences between these third order results and those obtained from the second order theory are attributed to the lack of coupling between modes which results from using a one-mode expansion.

The results obtained using an expansion consisting only of the 1R mode will now be summarized. As seen from Fig. (14) the pressure waveforms resemble sinusoids which are shifted up (for radial positions near the axis, $r = 0$) or down (for stations near the wall, $r = 1$). Figure (15) shows the dependence of the limit cycles upon n and $\bar{\tau}$. Unlike the 1T mode, stable limit cycles for 1R instability were found in the vicinity of the neutral stability limit for both linearly stable and linearly unstable values of n and $\bar{\tau}$. For an engine operating in the linearly stable region an unstable limit cycle (i.e., triggering limit) was found with an amplitude below that of the stable limit cycle. Also predicted is the minimum value of n (for a given $\bar{\tau}$) below which it is impossible to trigger combustion oscillations. The curves shown in Fig. (15) show that as $\bar{\tau}$ is increased, combustion oscillations are more easily triggered and the amplitude of the resulting oscillations is higher. It is also seen that the unstable range in n, for which triggering of combustion instability is possible, becomes larger with increasing values of the time-lag. These solutions are qualitatively similar to those obtained for the 1R mode using the second order theory and a one-mode expansion (see Ref. 1).

In the study of the 1R mode, the effect of various nonlinear terms appearing in the governing equations was evaluated. From the results of this study it was concluded that the nonlinearities in the combustion mass source are very important in determining the limiting

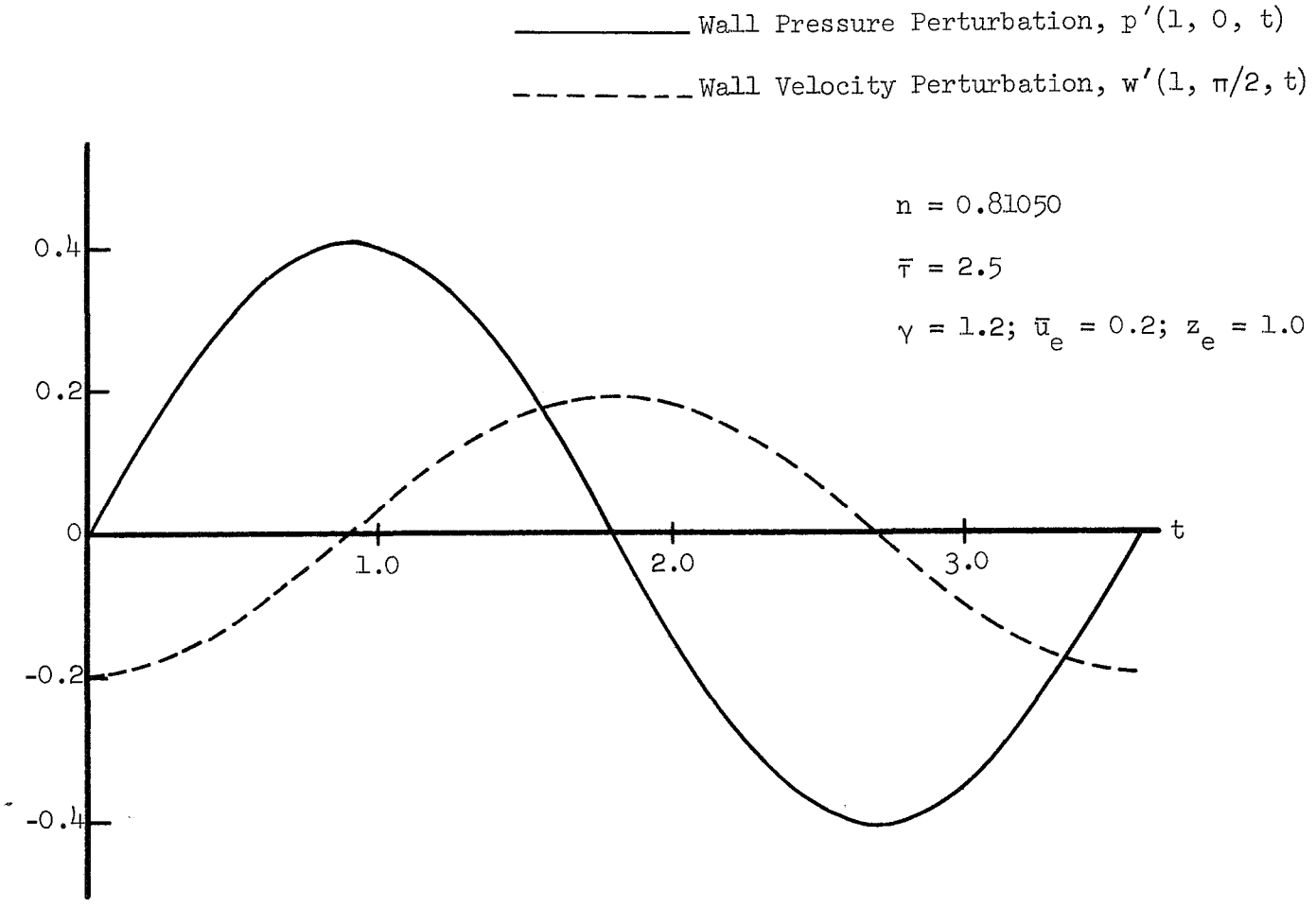

Figure 11. Third Order Wall Pressure and Velocity Waveforms for the 1T Mode at an Unstable Limit Cycle.

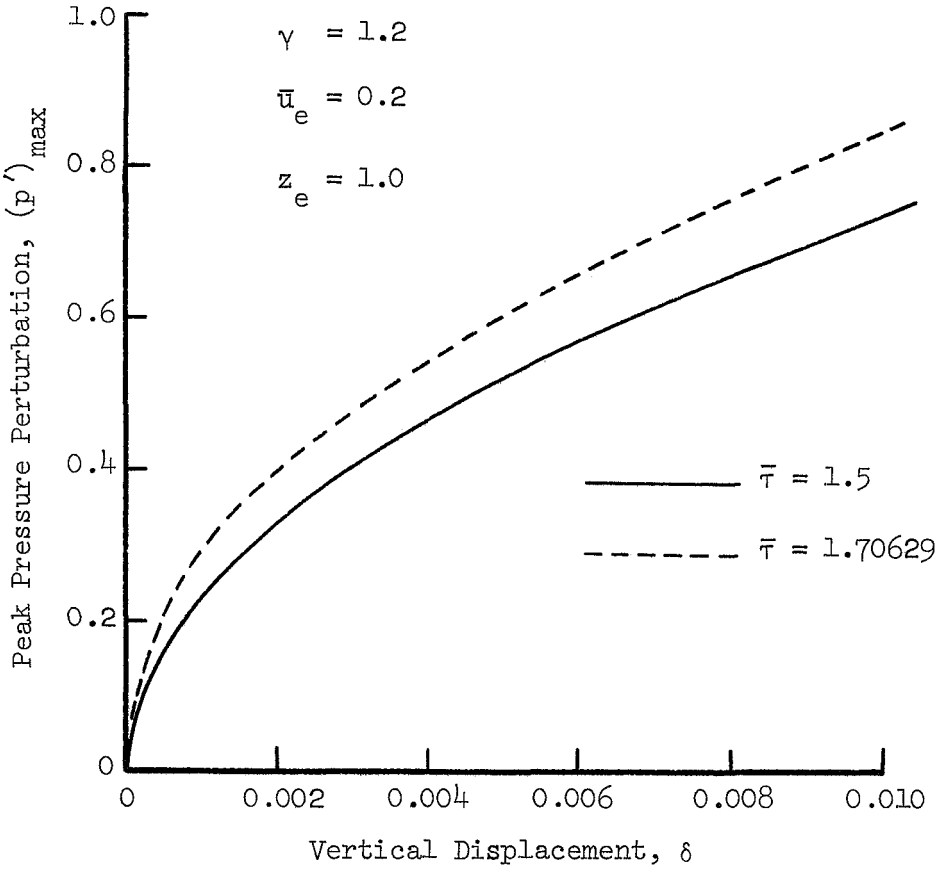

Figure 12. Third Order Stable Limit Cycles for the First Tangential Mode.

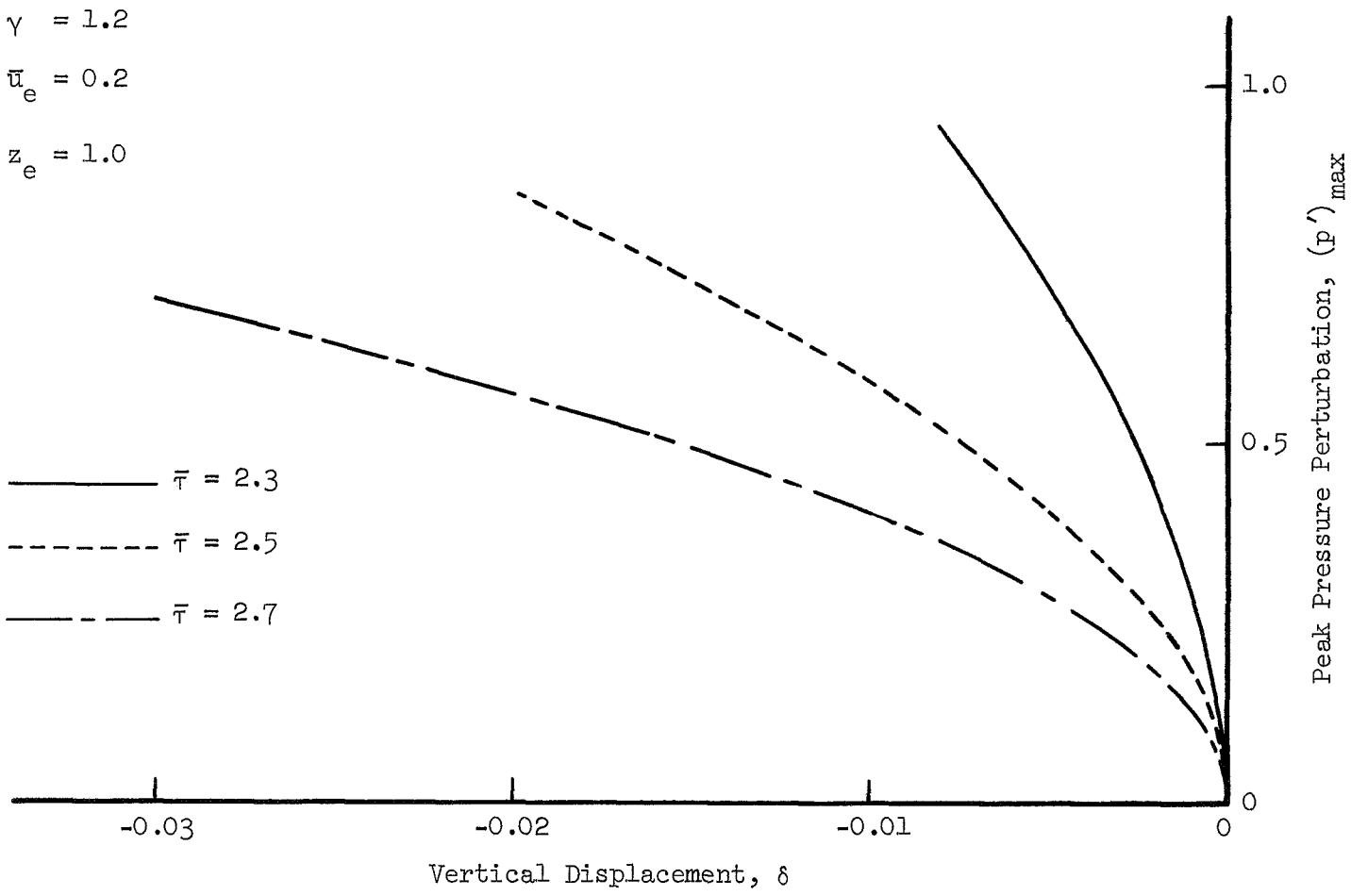

Figure 13. Third Order Triggering Limits for the First Tangential Mode.

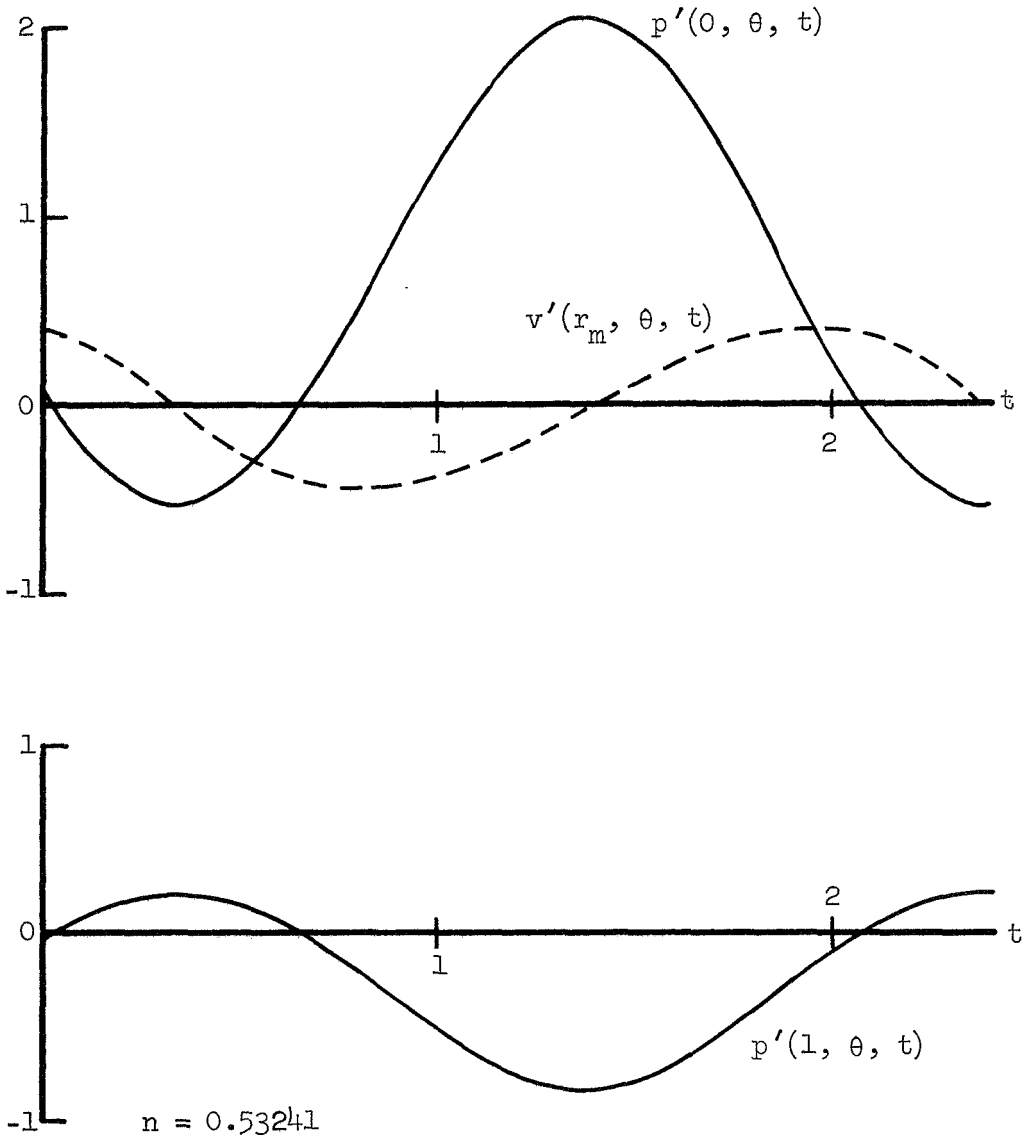

Figure 14. Third Order Pressure and Velocity Waveforms for the 1R Mode at a Stable Limit Cycle.

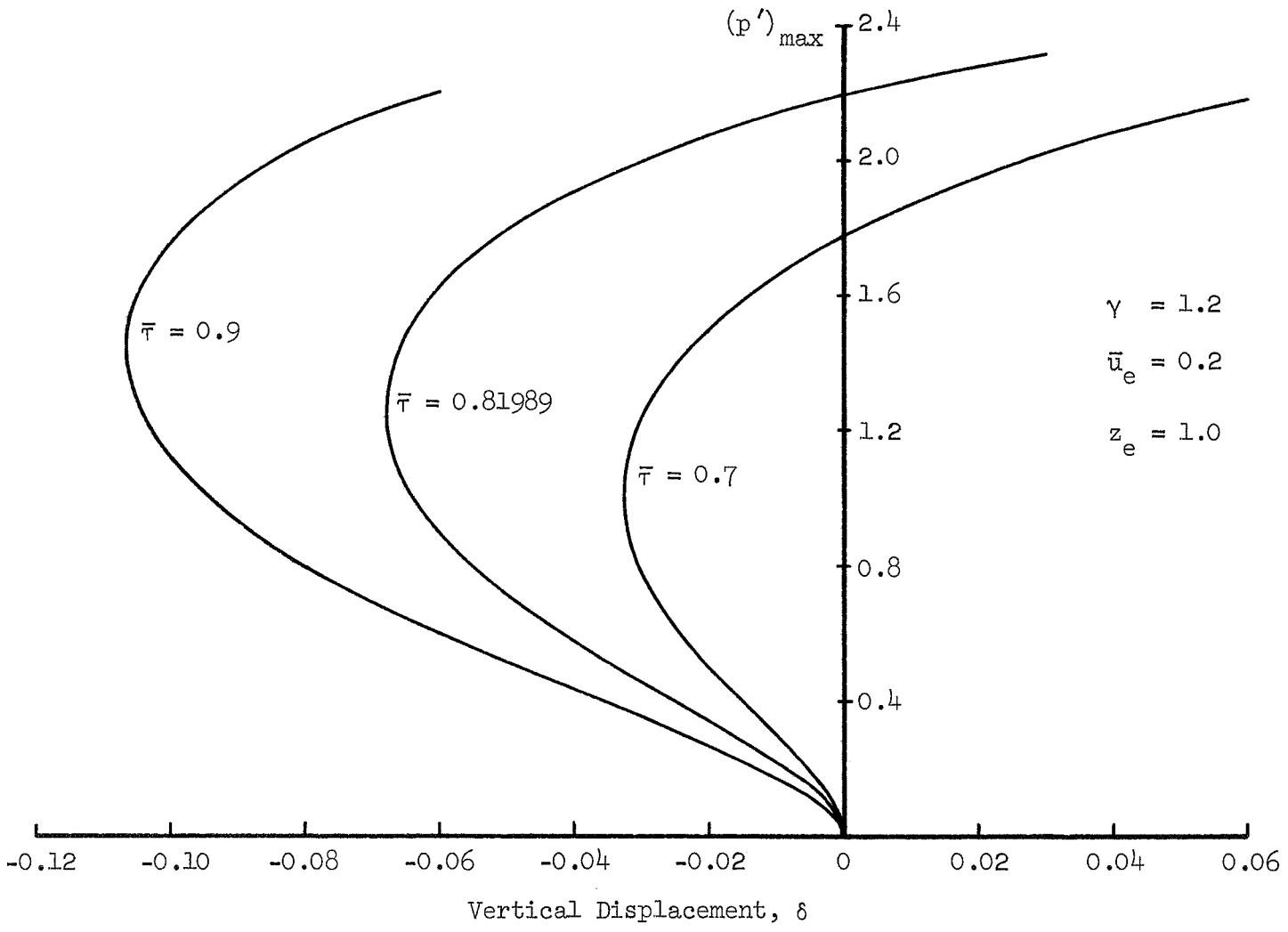

Figure 15. Third Order Stable and Unstable Limit Cycles for the First Radial Mode.

amplitude of triggered 1R mode instability. On the other hand the cubically nonlinear terms originating from the gasdynamics of the problem have only a minor effect.

Some of the third order solutions predicted the anomalous result that under certain conditions the combustor's pressure may become negative. The occurrence of negative pressures in the approximate solutions is a result of the assumed spatial dependence of the series solutions. To overcome this shortcoming work is presently in progress to develop a multi-mode third order theory.

Nonlinear Axial Mode Instability

In a separate study, the case of axial type instability in a combustor with a distributed combustion process is currently being investigated. Difficulties were encountered in the early stages of the study, but it now appears that they have been resolved. The work done to date will now be briefly summarized.

The nonlinear partial differential equation governing longitudinal combustion oscillations, correct to second order, is given by:

$$\Phi_{zz} - \Phi_{tt} - 2\Phi_z\Phi_{zt} - (\gamma-1)\Phi_t\Phi_{zz} - 2\bar{u}\Phi_{zt} - \gamma\frac{d\bar{u}}{dz}\Phi_t - W_m' = 0 \qquad (12)$$

In Eq. (12) the mass source term is again described by Crocco's time-lag hypothesis to give:

$$W_m' = -\gamma n\frac{d\bar{u}}{dz}\left[\Phi_t(z,t) - \Phi_t(z,t-\bar{\tau})\right] \qquad (13)$$

The appropriate boundary conditions arise from the presence of a solid wall boundary condition at the injector face ($z = 0$) and a quasi-steady nozzle at $z = 1$. The boundary conditions are given by:

$$\Phi_z(0) = 0 \tag{14}$$

$$\Phi_z(1) = -\frac{\gamma-1}{2}\bar{u}_e\Phi_t(1) \tag{15}$$

In order to obtain an approximate solution of Eq. (12) a series expansion must be specified for $\Phi(z,t)$; that is, $\tilde{\Phi} = \sum_{k=0}^{N} B_k(t)\varphi_k(z)$. The initial phases of this investigation have been primarily concerned with the proper selection of the approximating functions $\varphi_k(z)$.

If the trial functions φ_k do not satisfy the boundary conditions, then the resulting error at the boundary condition must be minimized, in some sense, in combination with the error arising from the fact that the trial function does not, in general, satisfy the differential equation. This is accomplished by imposing the following restriction (see Ref. 2):

$$\int_V R_E\varphi_k dV - \int_S R_B\varphi_k dS = 0 \tag{16}$$

where the residuals R_E and R_B are the errors incurred by substituting the approximate solutions into the differential equations and boundary conditions respectively. If the trial functions satisfy the boundary conditions then the residual R_B vanishes. Both approaches are currently under study, although most of the work done to date has been with trial solutions that do not satisfy the boundary conditions.

Obviously, a proper choice of the trial functions is a prerequisite for obtaining valid results. The first trial series for $\Phi(z,t)$ was taken to be composed of the following acoustic modes:

$$\Phi(z,t) = \sum_{k=0}^{N}\left[A_k(t)\sin(k\pi z) + B_k(t)\cos(k\pi z)\right] \tag{17}$$

This expansion does not satisfy either the injector or the nozzle boundary conditions. Using Eq. (16) yields a set of coupled nonlinear ordinary differential equations to be solved for the A_k's and B_k's. Numerical calculations proved this trial series to be divergent for all the investigated cases (i.e., all investigated values of n, $\bar{\tau}$).

Considerations of the expected physical behavior of the resulting pressure oscillations suggested the omission of the sine terms from the expansion given by Eq. (17), hence:

$$\Phi(z,t) = \sum_{k=0}^{N} B_k(t)\cos(k\pi z) \tag{18}$$

Preliminary results using this cosine series are favorable. The time dependent coefficient, $B_o(t)$ corresponding to the spatially uniform term in the series (i.e., $\varphi_o = 1$) was found to oscillate with a lower frequency than the remaining terms, but with a larger amplitude. This term corresponds to chugging-type instability. Results with and without this term present in the series expansion will be obtained; a comparison of these results with available experimental data will determine whether $B_o(t)$ should be included in the approximate series solution.

The second approach taken in selecting an approximate solution was to construct expressions that satisfy both the boundary condition at the injector face (i.e., z = 0) and that at the nozzle entrance (i.e., z = 1). Two methods are presently under consideration. One such method is to select an approximate solution of the form:

$$\Phi(z,t) = A(t)F(z) + G(z) \sum_{k=0}^{N} B_k(t)\cos(k\pi z) \tag{19}$$

where the summation term satisfies homogeneous boundary conditions and the remaining term A(t)F(z) satisfies both boundary conditions. For example, one such solution was found to be:

$$\Phi(z,t) = z^2 \exp\left[-2t/\beta\right] + z^2(z-1)\sum_{k=0}^{N} B_k(t)\cos(k\pi z) \qquad (20)$$

where $\beta = \frac{\gamma-1}{2}\bar{u}_e$. It should be noted that the first term is necessary to satisfy the nozzle admittance condition, but its effect on $\Phi(z,t)$ decreases with time.

The second method of satisfying the boundary conditions is to use a cosine series with time dependent "eigenvalues" as follows:

$$\Phi(z,t) = \sum_{k=0}^{N} B_k(t)\cos\left\{[k\pi + \epsilon_k(t)]z\right\} \qquad (21)$$

The above expression satisfies the boundary condition at $z = 0$. Applying the boundary condition at $z = 1$ (i.e., Eq. (15)) yields the following relation between $B_k(t)$ and $\epsilon_k(t)$:

$$\left[k\pi + \epsilon_k(t) + \beta\frac{d\epsilon_k}{dt}\right]B_k(t)\tan\epsilon_k(t) - \beta\frac{dB_k}{dt} = 0 \qquad (22)$$

Combining Eqs. (22) with the equations resulting from applying Eq. (16) results in a system of $2(N+1)$ nonlinear ordinary differential equations for the $2(N+1)$ unknowns, $\epsilon_k(t)$ and $B_k(t)$.

At present this investigation is at a preliminary stage, hence no numerical results are available. Computer programs are being developed based upon the three approaches discussed above. These will be used to determine both the linear and nonlinear stability limits in the $(n, \bar{\tau})$ plane and to study the possibility of triggering axial combustion oscillations.

Combustion Response Studies

With a view in mind to determine a more realistic combustion

response function for incorporation into the Galerkin method two detailed studies were carried out concerning combustion processes. The first study concerned the linear acoustic response of the vaporization process in the vicinity of the stagnation point[3]; the major difference from previous treatments was the assumption of no internal liquid circulation and the consequent existence of a thermal wave in the liquid in the steady state. The reasons for doing this study were that the thermal wave assumption had never been used before and it is precisely the thermal wave which is responsible for combustion response peaks in the appropriate frequency range in solid propellant response theory. A sample frequency response plot for two fuels is shown in Fig. (16). To draw this plot three items concerning the acoustics must be specified - the mode type, the position of the droplet in the chamber and the relative velocity direction between the chamber gases and the droplet. While Fig. (16) is a representative average for a longitudinal mode, significant differences can appear for transverse modes. The major item, however, is that the frequency response is fairly flat even though there is mild variation in the frequency range of interest to instability. This relatively flat behavior is in accord with treatments of the vaporization process using assumptions different than those used in the present study.

A second study concerned the effects of combustion process velocity sensitivity on stability[4]. There has been a general lack of recognition of the velocity effect's importance and it is believed that a reconciliation between two presently accepted but different instability theories can be affected by more detailed understanding of the velocity effect. Figure (17) demonstrates that a combustion rate instantaneously proportional to velocity raised to some power n can cause longitudinal instability; Ψ is the location of a concentrated combustion front expressed as a fraction of the chamber length. While the required n value is high (> 1) the demonstration is that velocity sensitivity is at least an important contribution to stability criteria.

The outcome of the above studies has been the recommendation of

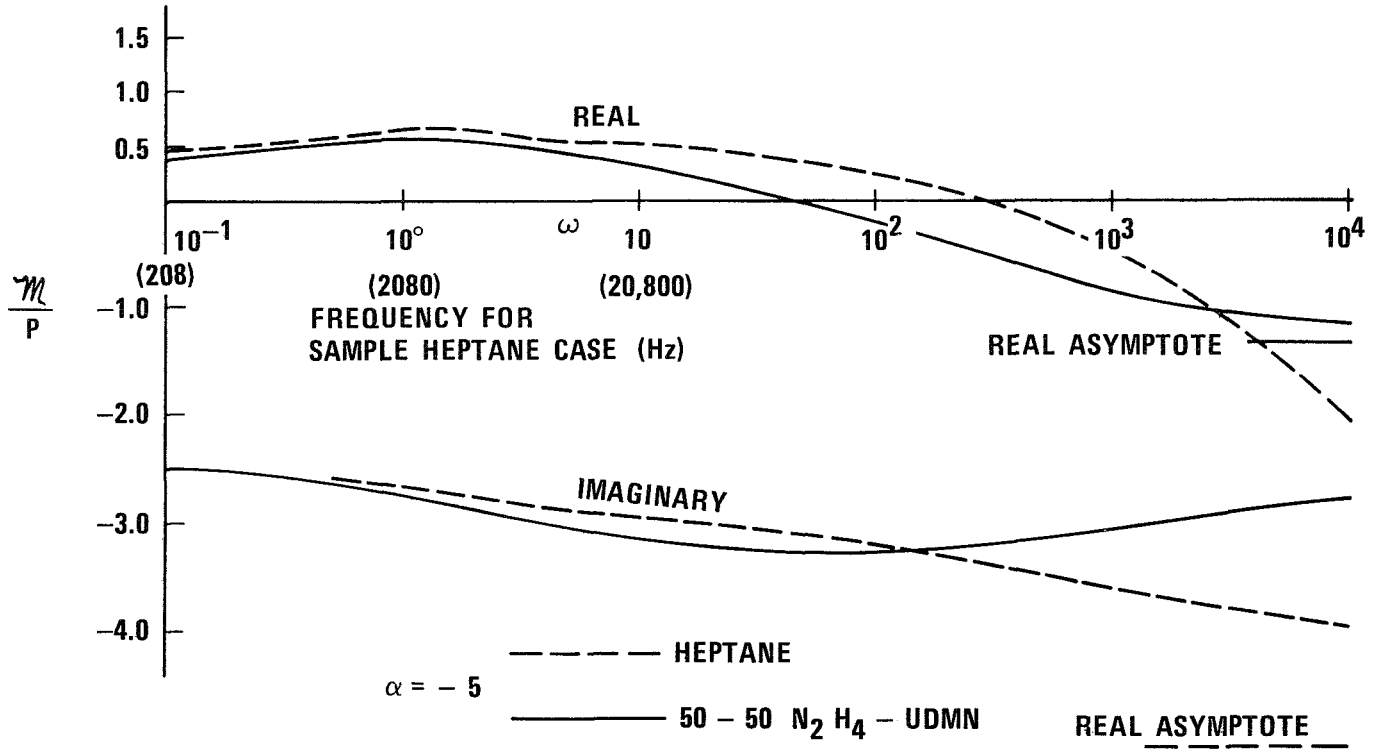

Figure 16. Frequency Response of Vaporization Process for Two Fuels.

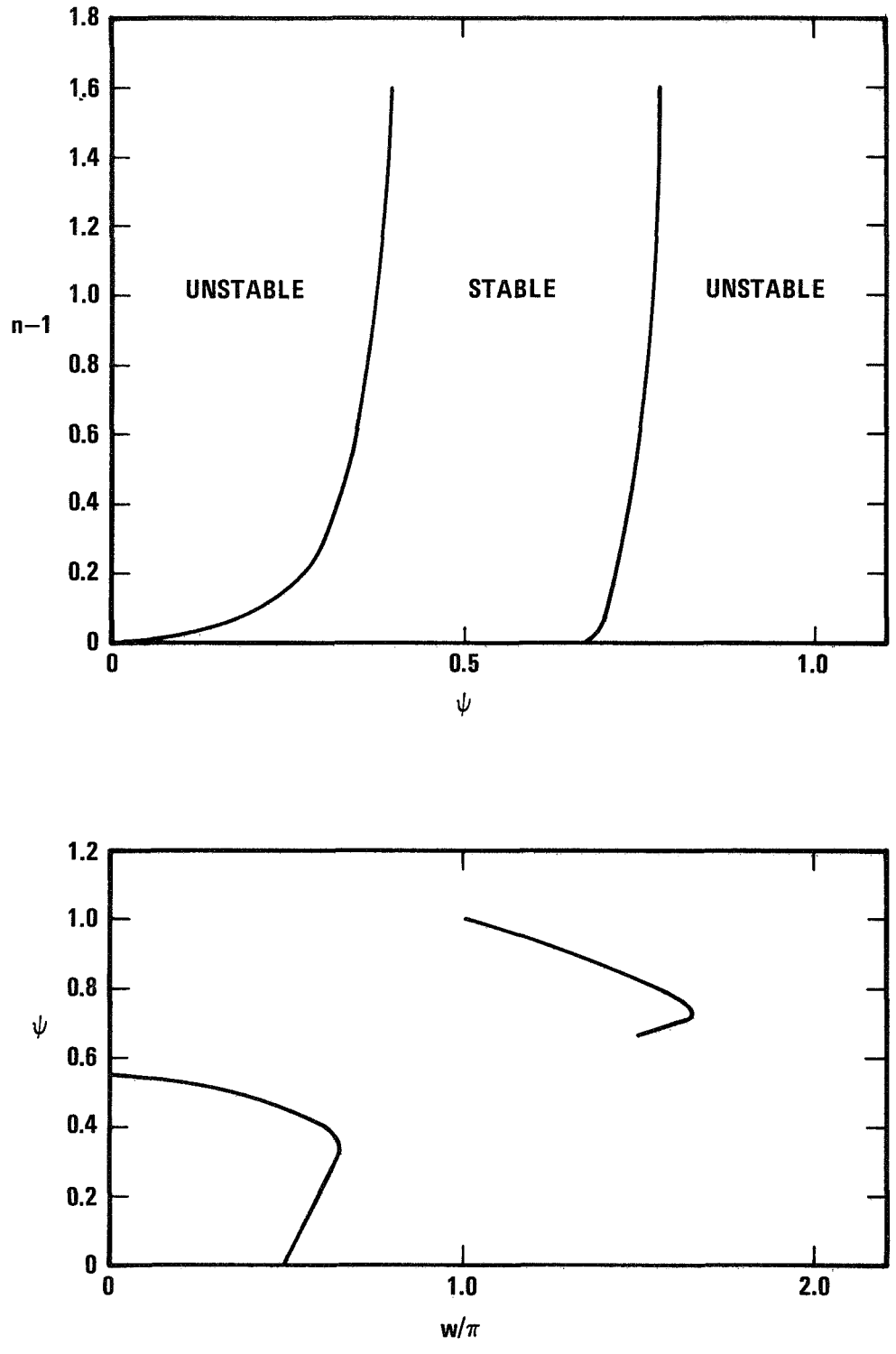

Figure 17. Stability Boundaries and Acoustic Frequencies for Velocity Effect Instability.

a new response function for incorporation into the Galerkin method[3]. This function consists of the sum of two terms - one describing the variable vaporization rate, which can include velocity effects, and one involving the variable combustion rate. It is shown in Ref. 3 that this formulation removes a rather critical assumption in the Crocco time lag theory.

Future Investigations

Future research efforts will be devoted to the following investigations: (1) determination of nonlinear stability limits using the second order theory, (2) determination of the characteristics of large amplitude transverse wave instability, (3) determination of the characteristics of nonlinear axial instability, and (4) investigation of the unsteady combustion response functions.

The second order computer programs that were developed to date are now being used to determine stability maps (similar to the one presented in Fig. 8) for rocket combustors characterized by various values of the Mach number and different length-to-diameter ratios. The possibility of using such maps together with experimental data, to determine the operating point (i.e., values of n and $\bar{\tau}$) of actual rocket motors will be explored. Additional investigations concerning the effect of initial conditions and the convergence of the assumed series expansions will be conducted. A report of the second order results, which includes a fully documented computer program, will be prepared in the near future.

The behavior of large amplitude transverse instability will be studied using a third order multi-mode theory which is currently under development. Results similar to those obtained with the aid of the second order theory will be obtained, and a comparison will be made with the second order results to determine the range of applicability of the second order theory.

Present efforts to determine the best analytical approach for the solution of the axial instability problem are expected to be completed shortly. Upon completion of this investigation the chosen method will be used to determine the nonlinear stability characteristics of various rocket combustors.

A nonlinear response function based on instantaneous high Reynolds number vaporization response will be incorporated into the second order theory. One of the objectives of this study is to compare triggering limits obtained by using the Galerkin method with the results obtained in Ref. (5). These results will also be compared with the previous second order results in order to determine differences in mode-excitation, magnitude of triggering amplitude, and limit cycle amplitude.

REFERENCES

1. Zinn, B. T., and Powell, E. A., "Application of the Galerkin Method in the Design of Stable Liquid Rocket Motors," Annual Report of Research Conducted Under NASA Grant NGR 11-002-083 for period August 1, 1968 to July 31, 1969, Georgia Institute of Technology.

2. Zinn, B. T., and Powell, E. A., "Application of the Galerkin Method in the Solution of Combustion Instability Problems," IAF paper p. 69, to appear in the Proc. 19th Congress of the Int. Ast. Federation.

3. Strahle, W. C., "New Considerations on Causes for Combustion Instability in Liquid Propellant Rockets," to appear in Combustion Science and Technology.

4. Strahle, W. C., "A Note on the Forgotten Velocity Effect in Combustion Instability of Liquid Rockets," to appear in Combustion Science and Technology.

5. Priem, R. J., and Guentert, D. C., "Combustion Instability Limits Determined by a Nonlinear Theory and a One-Dimensional Model," NASA TN D-1409, October, 1962.

6. Zinn, B. T., and Powell, E. A., "Nonlinear Combustion Instability In Liquid Propellant Rocket Motors," to be presented at the 13th Int. Symp. on Combustion, Salt Lake City, Utah, August, 1970.